Research Article | Vol. 11, No. 4 / 1 April 2020 / Biomedical Optics Express 1892
Biomedical Optics EXPRESS

Peripheral image quality in pseudophakic eyes

KONSTANTINA A. TOGKA,[1] ANGELOS LIVIR-RALLATOS,[1] DIMITRIOS CHRISTARAS,[1,2,*] SPYRIDON TSOUKALAS,[1] NIKOLAOS PAPASYFAKIS,[1] PABLO ARTAL,[3] AND HARILAOS GINIS[1]

[1]*Department of Research, Athens Eye Hospital, Leof. Vouliagmenis 45, Glifada 166 75, Greece*
[2]*UCL Institute of Ophthalmology, University College London, London, UK*
[3]*Laboratorio de Óptica, Instituto Universitario de Investigación en Óptica y Nanofísica, Universidad de Murcia, Campus de Espinardo, E-30100 Murcia, Spain*
[*]*d.christaras@athenseyehospital.gr*

Abstract: The purpose of this work was to evaluate peripheral image quality in the pseudophakic eye using computational, physical, and psychophysical methods. We designed and constructed a physical model of the pseudophakic human eye with realistic dimensions using a corneal phantom and a board-only camera that was pivoted around an axis that matched the anatomical center of a human retina, assuming a radius of curvature of 12 mm, while it was submersed in a 23.4 mm long water filled chamber to emulate human ocular axial length. We used this optical setup to perform direct recording of the point spread function (PSF) and the associated retinal images for a commercial intraocular lens (IOL). Additionally, psychophysical tests were carried out to investigate the impact of the off-axis astigmatism in peripheral visual performance, where spectacle-induced astigmatism simulated the pseudophakic conditions in healthy subjects. Our findings using the physical eye model confirm the existence of large amounts of astigmatism in the periphery of the pseudophakic eye. The psychophysical tests revealed a significant reduction of detection sensitivity in the peripheral visual field. The latter suggests that off-axis astigmatism in patients implanted with IOLs may have performance and safety implications for activities requiring efficient peripheral vision.

1. Introduction

The crystalline lens is a complicated structure and its function has been a topic of study for centuries. It exhibits a gradient refractive index from 1.390 at the lens surface to 1.409 at its core [1], achieved by an increasing concentration of crystalline proteins in the cytoplasm of lens fiber cells [2]. Despite the high presence of proteins, the healthy eye lens shows a remarkable transparency [3]. Furthermore, the lens shape is aspheric leading to reduced total spherical aberration by partially compensating the corneal spherical aberration [4,5]. It is interesting to note that the eye's optics resembles a wide-angle design such that the quality of the peripheral image on average exceeds the resolution limit imposed by the retina [6–8].

Intraocular lenses (IOLs) have been used in ophthalmology for more than half a century, since Harold Ridley inserted the first one to treat cataracts [9]. Lens implantation has since become the most common and successful surgery in ophthalmology. The implant is chosen such that it provides the necessary refractive power to optimize focus at the eye's fovea, substituting in this way the patient's crystalline lens. The central visual field of the pseudophakic eye shows generally good image quality [10], limited practically only by the residual postoperative sphero-cylindrical refractive errors and in some cases spherical aberration depending on the type of the IOL used [11,12].

Peripheral optical quality has traditionally been considered less important in vision and especially in terms of visual acuity [13,14]. Indeed, the density of the photoreceptors decreases

#387254 https://doi.org/10.1364/BOE.387254
Journal © 2020 Received 3 Jan 2020; revised 27 Feb 2020; accepted 1 Mar 2020; published 11 Mar 2020

Biomedical Optics EXPRESS

and neural convergence increases at larger eccentricities, leading to a higher sensitivity at the fovea falling rapidly towards the periphery at photopic conditions [15].

The above retinal limitations have led IOL manufacturers to design the implants considering mainly the image quality at small angles around the fovea and overlook their optical performance at the periphery. There are, however, specific visual tasks where peripheral optical quality has an impact on functional vision, for instance when detecting the direction of movement of a high spatial frequency grating in the periphery, or simpler tasks, like the detection of gratings [16,17]. This can have implications in visually demanding everyday tasks such as driving, where peripheral vision has been linked to driving [18–20]. Bower *et al.* found that even a mild to moderate restriction in the visual field, assessed by Goldman perimetry, can have a significant effect on driving [18].

There is some evidence [21,22] indicating that current IOLs do not provide peripheral image quality as good as that of the natural crystalline lens. Being designed specifically around surgical technique and aiming to restore emmetropia on the optical axis, IOLs are associated with increased astigmatism and higher order aberrations at the periphery of the visual field of the pseudophakic eye. The objective of this work was to further evaluate the peripheral optical quality of the pseudophakic eye.

In this work, we present an artificial eye model as a platform for qualitative and quantitative IOL testing in realistic conditions in the periphery of the visual field. The physical model is validated computationally by using a ray-tracing software. Using the results of the physical and computational simulations we also performed visual experiments to demonstrate the effects of spectacle-induced astigmatism in healthy subjects at the magnitude measured in the periphery of the pseudophakic eye.

2. Methods

2.1. Ray tracing

The optical characterisation of the wide-angle pseudophakic eye was initially done using raytracing in OpticStudio (Zemax LLC, Redmond, WA). The pseudophakic model was based on a previously reported wide-angle model of the human eye [23], where the crystalline lens was replaced with a bi-convex acrylic lens (refractive index: 1.55) of equivalent refractive power. A schematic of the phakic and the pseudophakic eye model can be seen in Fig. 1.

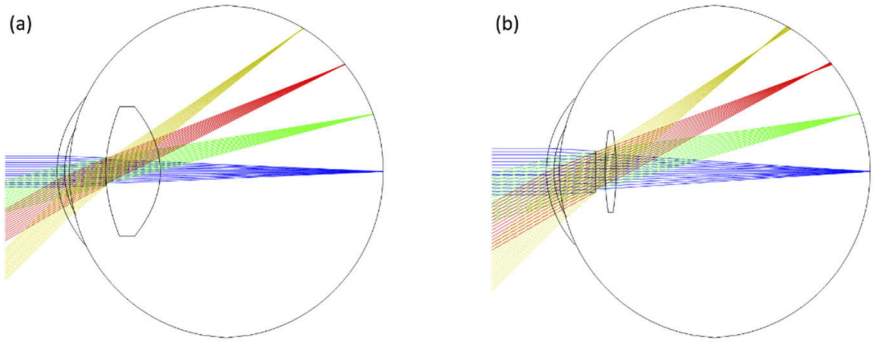

Fig. 1. Model for the natural eye (a) and the pseudophakic eye (b). Notice the change in field curvature in the periphery of the pseudophakic eye and the physical shape of the IOL compared to the natural lens.

The amount of astigmatism for each field angle was estimated by introducing an ideal spherocylindrical lens at the spectacle plane (12 mm from the cornea) and optimizing the

Biomedical Optics EXPRESS

modulation transfer function for each field angle. The difference between the sagittal and tangential powers determined the astigmatism.

2.2. Artificial eye

We designed and constructed a realistic artificial eye model to investigate the peripheral optics of the pseudophakic eye by directly recording the images of a point source (PSF) at four field angles and a wide-field image of a target. A schematic view of the eye is shown in Fig. 2.

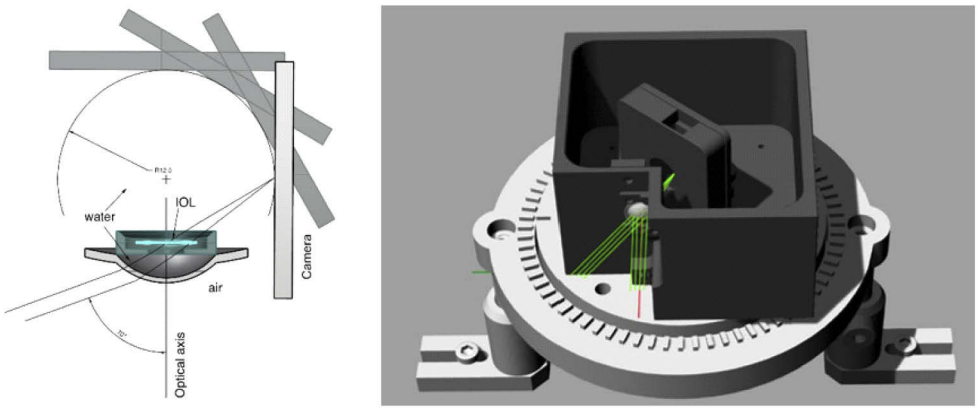

Fig. 2. Schematic (left) and 3D rendering (right) of the constructed artificial eye. The camera detector is submerged in water and can be rotated at various field angles. The artificial eye is mounted on top of a rotational stage which allows rotation of the entire system in a 5 degrees step.

The artificial eye was filled with water and includes a custom-made meniscus lens (EyeArt Laboratories; Thessaloniki, Greece) acting as the cornea. The anterior surface resembled the anterior surface of a human cornea both in base curvature and asphericity. Its anterior radius of curvature was equal to 7.73 mm and its conic constant was -0.26. The posterior curvature was adjusted to compensate for the difference of the refractive index of PMMA (n=1.49 at 546 nm) from that of the cornea (n=1.37 at 546 nm). The geometric characteristics of the cornea lens can be seen in Fig. 3. An 8-bit CMOS camera (DFM 72BUC02-ML, Imaging Source; Bremen, Germany) with a maximum native resolution of 2592×1944 pixels enclosed in a water-tight housing with a glass window having a thickness of 200μm with its sensor in contact with the glass. The camera was submersed in the water-filled chamber at the retina plane, 23.4 mm from the corneal apex. The camera had a pixel size equal to 2.2 μm, comparable to the mean foveal cone size [24]. The camera could be pivoted around an axis, passing through the anatomical center of the retina (denoted with a cross in Fig. 2, left), assuming a radius of curvature equal to 12 mm. The overall distance of the sensor plane from the cornea could be adjusted around the nominal value of 23.4 mm in order to focus the system for IOLs of different dioptric power.

An IOL was supported by its haptics in a receptacle posteriorly to the diaphragm (Fig. 3, right). The vertex of the anterior surface of the IOL was positioned at a distance of 4.4 mm from the vertex of the anterior surface of the cornea. The pupil diameter was 2.65 mm, corresponding to an entrance pupil of 3 mm in diameter. A biconvex hydrophobic acrylic IOL with 22D power (AcrySof SA60AT, Alcon Inc.) was used in this study. Pivoting the camera allowed testing for field angles ranging from 0 to 60 degrees. The artificial eye was mounted on a rotating stage allowing a 180 degrees rotation with a step of 5 degrees.

The PSF of the system was recorded by imaging the tip of a multimode fiber optic (0.2 mm), positioned at a distance of 4 m from the artificial eye. The fiber was emitting broadband (white)

Biomedical Optics EXPRESS

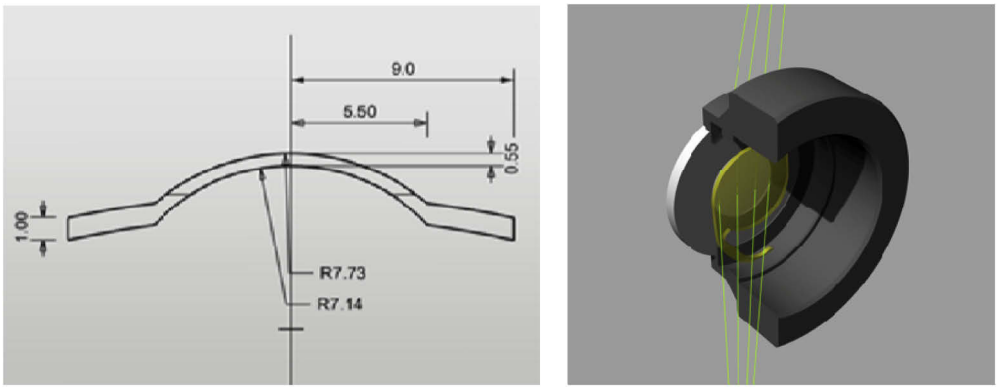

Fig. 3. Geometrical parameters of the artificial eye's cornea (left) and 3D rendering of the IOL holder.

light, coupled from an incandescent lamp (T=3500 K). The calculated geometrical image of the fiber tip on the sensor plane was smaller than that of a single pixel. Peripheral PSF was acquired by rotating the artificial eye on its rotating stage to the desired angle and pivoting the camera around the anatomical axis so that the image of the fiber tip was brought to the center of the sensor (see Fig. 2, right). The total axial length was adjusted to achieve on-axis best-focus by maximising the peak intensity of the spot for each eccentricity, in this case at 0, 15, 30 and 45 degrees of visual angle. Following this step, peripheral astigmatism at each eccentricity was assessed by maximising peak intensity using cylindrical trial lenses mounted on a holder at 12 mm from the corneal plane.

As an additional, qualitative test, a set of images showing optotypes on a computer screen were recorded at 0, 10, 20, 30 and 40 degrees.

2.3. Peripheral vision testing

We developed a psychophysical test to evaluate the impact of peripheral astigmatism on vision. The test pertained to the estimation of the differential detection threshold on phakic subjects at normal and simulated pseudophakic conditions, achieved with the use of cylindrical trial lenses to simulate the additional refractive error caused by an intraocular lens. The appropriate power of the trial lens was determined using the physical eye model described above, subtracting the astigmatism of the natural eye found in the computations.

The psychophysical test estimated the detection threshold of the subject at 15 and 45 degrees of visual angle with and without induced cylinder using cylindrical trial lenses mounted at a distance of 12 mm from the subject's eye. For the psychophysical task we used the adaptive staircase technique. First, the subject fixated on a target on the optical axis shown on the monitor, positioned at 450 mm from the subject (Fig. 4).

A 30 arcmin (comparable to Goldmann size III), grey, round stimulus was displayed, located at 15 or 45 degrees of the subject's visual field, accompanied by a sound. The task started with the stimulus at a high luminance so that it was always detected by the subject and decreased at a fixed step, until the subject was no longer able to detect it. The luminance of the stimulus then increased at a fixed step, until the subject was once again able to detect it and the direction of luminance changed once again. The task ended after four such inversions and the value of the threshold was taken to be the average of these four values. In order to reduce the statistical weight of false positives or negatives we allowed two consecutive replies of the same kind before changing the direction of the luminance. For the experiment a purposely-built MATLAB script and a graphical user interface (GUI) were used. For the presentation of the stimuli MATLAB's

Biomedical Optics EXPRESS

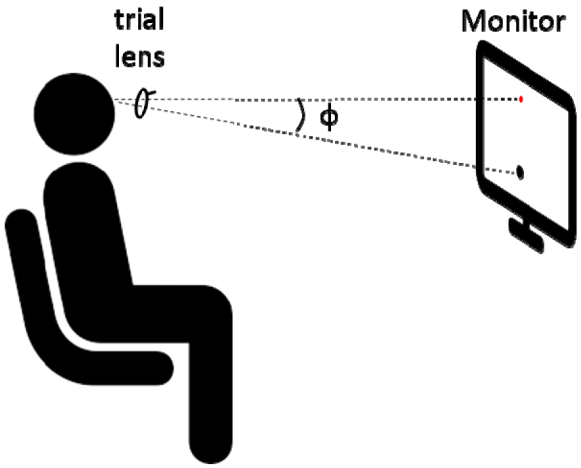

Fig. 4. Schematic of the psychophysical experiment. The trial lens was used to simulate the pseudophakic eye at φ=15° and φ=45°.

Psychophysics toolbox [25] was used. During the evaluation of the control experiment (heathy eye) we introduced a trial lens of -0.25D to incorporate reflection losses at the trial lens. The background luminance was set to 13.35 cd/m^2 and the subject was allowed to adapt to that luminance through training trials.

Eleven healthy volunteers, 5 males and 6 females, with no known ophthalmic pathology were enrolled in the measurements described above after they had been informed about the nature of the study and had provided an informed consent. The central refractive error was assessed psychophysically and was smaller than 1D for all 11 subjects. Minimum pupil size at the conditions of the experiment was 4 mm. The mean age was 24.9 (std=8).

3. Results

Ray tracing analysis showed that for the natural eye a vertical cylinder of about 4.15 D was needed to maximize the MTF. For the pseudophakic model the respective value was 9.85 D. The value for the phakic eye was consistent with previous experimental data [26,27]. The corresponding spot diagrams at 45 degrees after correcting with the appropriate amount of cylinder are presented in Fig. 5. The resulting cylinder difference between the phakic and the pseudophakic eye at 45 degrees, calculated using ray tracing, was found to be 5.7 D.

Images in the central and the peripheral visual field were recorded using the physical eye model mounted with the IOL as described in the methods section. Figure 6 shows a set of such images corresponding to the field between 0 and 40 degrees as recorded in the artificial eye.

The point spread function (PSF) was recorded at 0, 15, 30 and 45 degrees using the physical eye model with the monofocal IOL (Fig. 7).

In order to determine the amount of astigmatism at 45 degrees of the pseudophakic eye, a set of trial lenses was used, placed in front of the physical eye model, until best image was achieved. It was concluded that a -10D cylindrical lens was needed to achieve best image, in accordance to the ray tracing analysis. This value for the magnitude of cylinder is higher than what is previously reported using Hartmann-Shack measurements [21]. This difference may be related to the fact that in the present raytracing analysis as well as physical model measurements the full elliptical pupil is considered. The image was refined for residual defocus by adjusting the eye's axial length. The image without and with cylindrical correction is shown in Fig. 8.

Biomedical Optics EXPRESS

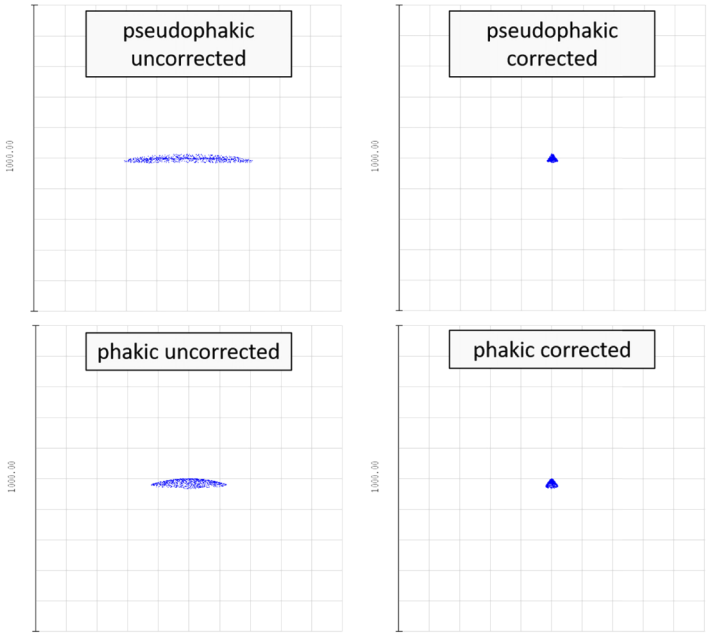

Fig. 5. Spot diagrams for the pseudophakic eye (top row) and the natural eye (bottom row), uncorrected (left column) and corrected for astigmatism (right column), at 45 degrees. The uncorrected size of the PSF in the phakic case is almost double in size horizontally.

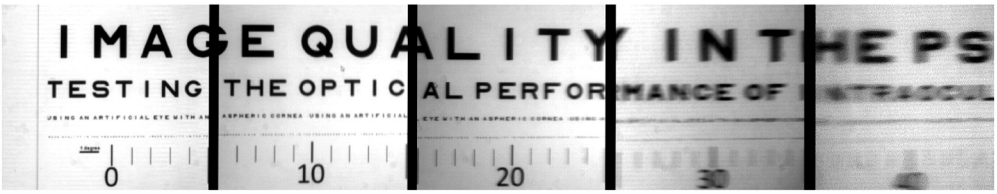

Fig. 6. Image quality degradation towards the periphery of the visual field of the pseudophakic eye (0-40 degrees).

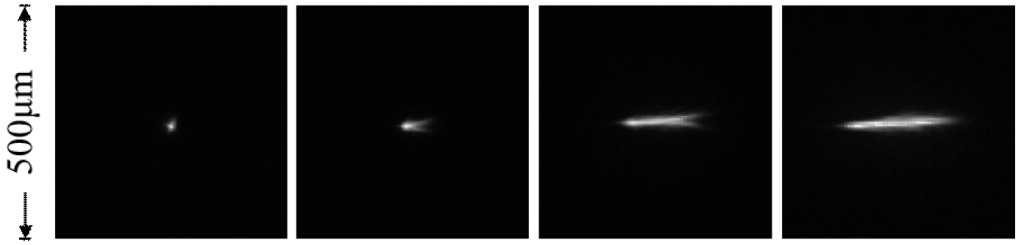

Fig. 7. Recorded PSFs (logarithm gray scale) for the IOL tested. Each image corresponds to a different eccentricity. From left to right: 0, 15, 30 and 45 degrees. Side of each image is 500µm on the camera plane, corresponding to 1.75 degrees of visual angle.

Biomedical Optics EXPRESS

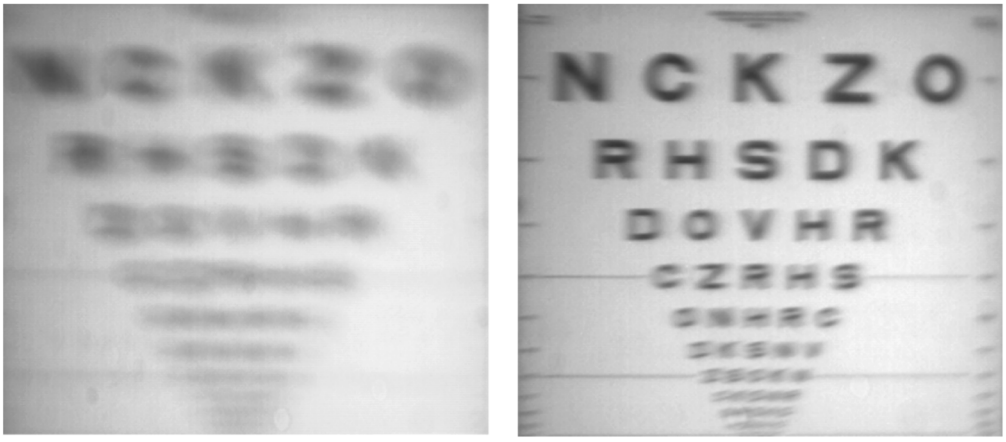

Fig. 8. Image captured at 45 degrees of visual angle with the physical eye model and the monofocal IOL, without cylindrical correction (left) and using a correcting cylindrical lens of -10D (right). The size of the letters of the first row is 1 degree.

The astigmatism expressing the difference between the phakic and the pseudophakic was determined using the simulations above, as explained in the methods section, and was found to be -1.5D and -6D at 15 and 45 degrees respectively, with the axis of the (positive) cylinder parallel to the sagittal plane for the off-axis stimulus. The corresponding sensitivity loss in dB with the induced cylindrical error at 15 and 45 degrees for the eleven subjects is shown in Fig. 9.

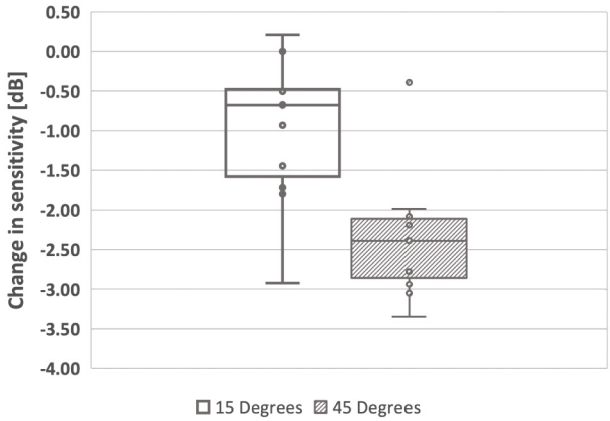

Fig. 9. Boxplot showing sensitivity loss in dB at 15 degrees (open) and 45 degrees (filled).

The mean sensitivity loss for all 11 subjects was found to be -0.98 ± 0.874 dB and -2.37 ± 0.754 dB at 15 degrees and 45 degrees respectively.

4. Discussion

Peripheral image deterioration in the pseudophakic eye has been assessed in the past in-vivo using a Hartmann-Shack sensor [21]. The purpose of this work is to quantify peripheral image quality in the pseudophakic eye through computational and physical simulations and, second, to demonstrate a visual task where the deteriorated peripheral image in the pseudophakic eye has visual impact.

Biomedical Optics EXPRESS

For the physical simulations, an artificial eye was developed and tested with a currently used monofocal IOL. The physical simulations for the monofocal lens support our original hypothesis that IOLs are optimized for central vision but offer poor peripheral image quality. The physical model was primarily designed to record peripheral retinal image quality. The detector can capture images at sampling frequencies sufficient for the analysis of visual phenomena ((Nyquist frequency >60 cycles/degree). However, this sampling frequency is not sufficient for the proper analysis of the central peak of the PSF and the calculation of the MTF especially in nearly diffraction-limited conditions where the size of the PSF can be comparable to the pixel size. This limitation does not exist in the mid and far periphery where the PSF is widened due to astigmatism and other aberrations and is sampled by several tens of pixels.

The effect of the decreased optical quality of the pseudophakic eye in vision was tested through the simulation of peripheral error in a group of healthy subjects, using appropriate trial lenses, corresponding to the error found in the computation and physical models for the normal and the pseudophakic eye. The visual task tested was the differential detection threshold with and without the induced astigmatism corresponding to the difference between the normal eye, as found computationally and the pseudophakic eye, determined in the physical eye model. All subjects exhibited decreased threshold sensitivity at the periphery due to the induced astigmatic error, showing the potential impact of a degraded peripheral optics in vision. Studies have reported that peripheral astigmatism shows great variability amongst the population [26,28] that could explain the large differences in sensitivity changes induced by the added cylinder. It is important to point out that we merely investigated the immediate reduction of sensitivity associated to the introduction of astigmatism in the peripheral visual field. It is unknown whether long term adaptation mechanisms can mitigate this effect.

The variability of ocular shape, especially in myopic eyes is such that the prediction of the exact ocular shape from common biometric data is not possible [29]. As one would expect, ocular shape affects significantly the image quality in the periphery, introducing large amounts of defocus in certain eyes.

Our results show that patients implanted with IOLs after cataract surgery may have a reduced sensitivity to detect small stimuli in the periphery. This may have consequences for navigation or orientation after cataract surgery with current IOLs.

5. Conclusions

Computational and physical modelling of the pseudophakic eye revealed high amounts of astigmatism in the periphery compared to the natural eye. Using a commercial monofocal IOL we found that the pseudophakic eye has approximately -6 D higher astigmatism at 45 degrees compared to the average natural eye. Psychophysical tests on healthy volunteers showed that this amount of astigmatism can reduce visual field sensitivity by 2.37 dB in the periphery. This effect might have implications in any daily task that involves detection of small objects in the periphery, such as navigation and driving.

Funding

National Strategic Reference Framework (T1EDK - 03913); European Research Council (AdG-2013-339228 SEECAT); Fundación Séneca (19897/GERM/15); Secretaría de Estado de Investigación, Desarrollo e Innovación (FIS2016-76163-R).

Disclosures

The authors declare no conflicts of interest.

Biomedical Optics EXPRESS

References

1. S. Kasthurirangan, E. L. Markwell, D. A. Atchison, and J. M. Pope, "In vivo study of changes in refractive index distribution in the human crystalline lens with age and accommodation," Invest. Ophthalmol. Visual Sci. **49**(6), 2531–2540 (2008).
2. P. P. Fagerholm, B. T. Philipson, and B. Lindström, "Normal human lens-the distribution of protein," Exp. Eye Res. **33**(6), 615–620 (1981).
3. M. Delaye and A. Tardieu, "Short-range oder of crystallin proteins accounts for eye lens transparency," Nature **302**(5907), 415–417 (1983).
4. P. Artal, A. Guirao, E. Berrio, and D. R. Williams, "Compensation of corneal aberrations by the internal optics in the human eye," J. Vis. **1**(1), 1 (2001).
5. P. Artal, E. Berrio, A. Guirao, and P. Piers, "Contribution of the cornea and internal surfaces to the change of ocular aberrations with age," J. Opt. Soc. Am. A **19**(1), 137 (2002).
6. D. R. Williams, P. Artal, R. Navarro, M. J. Mcmahon, and D. H. Brainard, "Off-axis optical quality and retinal sampling in the human eye," Vision Res. **36**(8), 1103–1114 (1996).
7. P. Artal, S. Marcos, R. Navarro, and D. R. Williams, "Odd aberrations and double-pass measurements of retinal image quality," J. Opt. Soc. Am. A **12**(2), 195–201 (1995).
8. L. Lundstrom, S. Manzanera, P. M. Prieto, D. B. Ayala, N. Gorceix, J. Gustafsson, P. Unsbo, and P. Artal, "Effect of optical correction and remaining aberrations on peripheral resolution acuity in the human eye," Opt. Express **15**(20), 12654–12661 (2007).
9. B. Jay, D. J. Apple, and J. Sims, "Remembrances of things past: Harold Ridley and the Invention of the Intraocular Lens," Surv. Ophthalmol. **40**(4), 279–292 (1996).
10. P. Artal, S. Marcos, R. Navarro, I. Miranda, and M. Ferro, "Through focus image quality of eyes implanted with monofocal and multifocal intraocular lenses," Opt. Eng. **34**(3), 772–779 (1995).
11. A. Guirao, M. Redondo, E. Geraghty, P. Piers, S. Norrby, and P. Artal, "Corneal Optical Aberrations and Retinal Image Quality in Patients in Whom Monofocal Intraocular Lenses Were Implanted," Arch. Ophthalmol. **120**(9), 1143–1151 (2002).
12. D. H. Chang and K. M. Rocha, "Intraocular lens optics and aberrations," Curr. Opin. Ophthalmol. **27**(4), 298–303 (2016).
13. Y. Z. Wang, L. N. Thibos, and A. Bradley, "Effects of refractive error on detection acuity and resolution acuity in peripheral vision," Invest. Ophthalmol. Visual Sci. **38**, 2134–2143 (1997).
14. M. Millodot, C. Johnson, A. Lamont, and H. Leibowitz, "Effect of dioptrics on peripheral visual acuity," Vision Res. **15**(12), 1357–1362 (1975).
15. E. Aulhorn and H. Harms, "Visual Perimetry," in *Visual Psychophysics*, D. Jameson and L. M. Hurvich, eds. (Springer: Berlin Heidelberg, 1972), pp. 102–145.
16. R. Rosén, L. Lundström, and P. Unsbo, "Influence of optical defocus on peripheral vision," Invest. Ophthalmol. Visual Sci. **52**(1), 318–323 (2011).
17. R. S. Anderson, "The selective effect of optical defocus on detection and resolution acuity in peripheral vision," Curr. Eye Res. **15**(3), 351–353 (1996).
18. A. Bowers, E. Peli, J. Elgin, G. McGwin, and C. Owsley, "On-road driving with moderate visual field loss," Optom. Vis. Sci. **82**(8), 657–667 (2005).
19. C. Owsley and G. McGwin, "Vision and driving," Vision Res. **50**(23), 2348–2361 (2010).
20. B. Wolfe, J. Dobres, R. Rosenholtz, and B. Reimer, "More than the Useful Field: Considering peripheral vision in driving," Appl. Ergon. **65**, 316–325 (2017).
21. B. Jaeken, S. Mirabet, J. M. Marín, and P. Artal, "Comparison of the optical image quality in the periphery of phakic and pseudophakic eyes," Invest. Ophthalmol. Vis. Sci. **54**(5), 3594–3599 (2013).
22. J. Tabernero, A. Ohlendorf, M. D. Fischer, A. R. Bruckmann, U. Schiefer, and F. Schaeffel, "Peripheral refraction in pseudophakic eyes measured by infrared scanning photoretinoscopy," J. Cataract Refractive Surg. **38**(5), 807–815 (2012).
23. R. Navarro, J. Santamaría, and J. Bescós, "Accommodation-dependent model of the human eye with aspherics," J. Opt. Soc. Am. A **2**(8), 1273 (1985).
24. C. A. Curcio, K. R. Sloan, O. Packer, A. E. Hendrickson, and R. E. Kalina, "Distribution of Cones in Human and Monkey Retina: Individual Variability and Radial Asymmetry," Science **236**(4801), 579–582 (1987).
25. D. H. Brainard, "The Psychophysics Toolbox," Spatial Vis. **10**(4), 433 (1997).
26. J. Gustafsson, E. Terenius, J. Buchheister, and P. Unsbo, "Peripheral astigmatism in emmetropic eyes," Oph. Phys. Optics **21**(5), 393–400 (2001).
27. J. Polans, B. Jaeken, R. P. McNabb, P. Artal, and J. A. Izatt, "Wide-field optical model of the human eye with asymmetrically tilted and decentered lens that reproduces measured ocular aberrations," Optica **2**(2), 124 (2015).
28. B. Jaeken and P. Artal, "Optical quality of emmetropic and myopic eyes in the periphery measured with high-angular resolution," Invest. Ophthalmol. Visual Sci. **53**(7), 3405–3413 (2012).
29. D. A. Atchison, C. E. Jones, K. L. Schmid, N. Pritchard, J. M. Pope, W. E. Strugnell, and R. A. Riley, "Eye shape in emmetropia and myopia," Invest. Ophthalmol. Visual Sci. **45**(10), 3380–3386 (2004).